

# OPERATIONAL CHARACTERISTICS OF THE TRISTAN ACCUMULATION RING VACUUM SYSTEM

T. Momose, K. Narushima, K. Kanazawa, H. Mizuno, H. Watanabe, and H. Ishimaru  
National Laboratory for High Energy Physics  
Oho-machi, Tsukuba-gun, Ibaragi-ken, 305, Japan

## Abstract

The operational characteristics of the TRISTAN vacuum system is described. The vacuum system is made of aluminum alloys<sup>1</sup> using specially extruded aluminum pipes. The best base pressure, on the order of  $10^{-8}$  Pa, was obtained without any baking or discharge cleaning. The thermal gas desorption rate of the aluminum chambers was on the order of  $10^{-10}$  Pa.l/s.cm<sup>2</sup>. For a time integrated beam current of 13.5 A.h, the pressure rise due to synchrotron radiation was  $2.1 \times 10^{-8}$  Pa/mA and the maximum beam lifetime was about 2 hours at several mA. The pressure rise is approximately inversely proportional to the time integrated beam current and is initially proportional to the beam energy, changing after about 7 A.h, to being proportional to the square root of the beam energy. A pressure independent lifetime of 357 min was observed. The lifetime at higher beam currents is proportional to the time integrated beam current. No thermal problems due to synchrotron radiation were observed. Corrosion due to high energy radiation in the presence of humidity was found in the aluminum windows for X-rays and  $\gamma$ -rays. Heating problems due to wall current discontinuities did not occur in the dual flat mirror surface seal type gate valves made of aluminum alloys. They were observed in a current transformer, in the ceramic chambers, and in a normal, Viton sealed gate valve.

## Introduction

The construction of the TRISTAN vacuum system (injection line and accumulation ring) was completed and the first beam was injected in October 1983. Beam was stored at 2.55 GeV in November and was accelerated to 5.2 GeV in December. In February 1984, operation using internal targets was started. In June, beam was accelerated to 6.5 GeV with the parallel operation of normal and superconducting cavities. At 2.55 GeV, maximum beam currents of 65 mA for single bunch and 90 mA for three bunches were obtained. Successful operation showed no substantial problem with this first all-aluminum alloy, ultra-high vacuum system.

## Accumulation Ring (AR)

### Pumps, Base Pressure, and Thermal Gas Desorption Rate

The AR, which has a circumference of 377 m, is divided by aluminum gate valves<sup>2</sup>. Roughing pumps are 12 turbomolecular pumps TMP(50 l/s) and 12 rotary pumps RP (250 l/min). The main pumps are 56 distributed ion pumps DIP(250 l/s) in the bending magnet chambers(2.5 m). The DIPs are made of aluminum alloys with Ti cathodes and can be operated at magnetic fields between 4 and 11 KG. Pumping speeds are about 100 l/s.m in the pressure range from  $10^{-7}$  to  $10^{-9}$  Pa. The sub-pumps are 70 sputter ion pumps SIP(30 l/s) and 70 non evaporable getters NEG (50 l/s). The SIPs are also made of aluminum alloys and their structure is nearly the same as the DIPs. The power supply for each SIP is a DC-DC converter<sup>3</sup>. There are two types of 5.5 kV power supplies, a 20 mA type for 500 l/s SIPs and DIPs, and a 5 mA type for 30 l/s and 10 l/s SIPs. A 2 unit NIM module contains one 20 mA type or two 5 mA types.

Three RF cavities are set in one of the 4 long straight sections. The RF cavities are not made of aluminum alloys but of mild steel electroplated with 0.1 mm thick Cu<sup>4</sup>. Each RF cavity has a roughing pump (250 l/s TMP and 250 l/min RP) and 2 SIPs(500 l/s) as a main pump. The total pumping speed is about 23000 l/s along the ring.

Each section was first evacuated by a roughing pump. At a pressure of  $10^{-4}$  Pa, NEG<sup>5</sup>s, operated in a room temperature mode, were activated. Then operation of the SIPs(30 l/s) was started. During the operation of the SIPs, no abnormal discharge was observed. The pressure of 8 sections in the arcs reached to  $10^{-6}$  Pa after one week's evacuation using only sub-pumps. Base pressure on the order of  $10^{-8}$  Pa was obtained using main pumps without any baking or discharge cleaning. Thermal gas desorption rate was on the order of  $10^{-10}$  Pa.l/s.cm<sup>2</sup> without baking. This is the same value obtained during bench test<sup>1</sup>. It must be mentioned that all the chambers, including the SIPs and DIPs, were virgin; helium leak checking was used.

Baking was done twice to a section which included 5 sets of quadrupole and bending magnets. The pressure change associated with the first baking is shown in Fig.1.

The pressure in the RF cavities reached the order  $10^{-6}$  Pa after evacuation of 10<sup>2</sup> hours using roughing and main pumps. To obtain less than  $10^{-7}$  Pa, the cavities had to be baked. After baking, the estimated thermal gas desorption rate of the cavities was on the order of  $10^{-10}$  Pa.l/s.cm<sup>2</sup>. RF conditioning was necessary to reduce the pressure rise during operation. Conditioning times were about 2 hours after the first one of 20 hours. During conditioning, the pressure in cavities was on the order of  $10^{-3}$  Pa. The main desorbed gas species were H<sub>2</sub>, CO, and CO<sub>2</sub>.

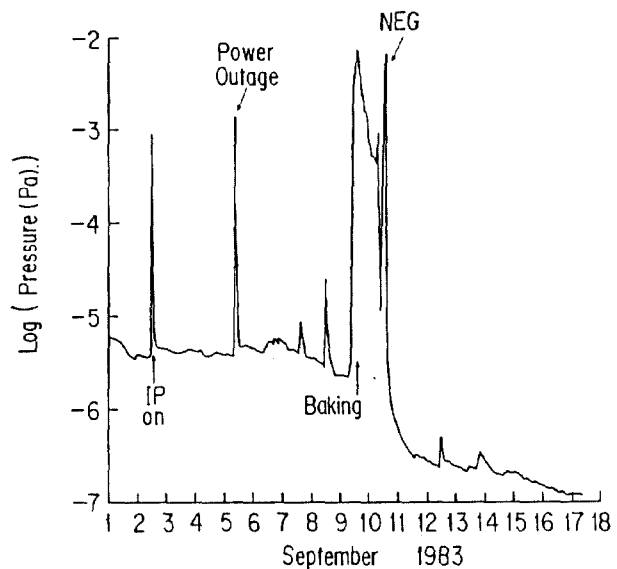


Fig.1 Initial pumping curve of a section in the AR.

## Dynamic Gas Desorption

The required pressure of  $10^{-8}$  Pa without beam was satisfied. However, the required pressure of  $10^{-7}$  Pa with beam was not satisfied because of the pressure rise due to synchrotron radiation; that is, photo-induced gas desorption(dynamic gas desorption). Fig.2 shows the pressure rise  $\Delta P/I$ (Pa/mA) and  $\eta$  as a function of the time integrated beam current  $D$ (mA.h). The data are based on the pressure of 8 sections in the arcs and are calculated using 1900 l/s as an average pumping speed for each section. After a time integrated beam current of 10<sup>2</sup> mA.h,  $\Delta P/I$  is approximately given by the equation,

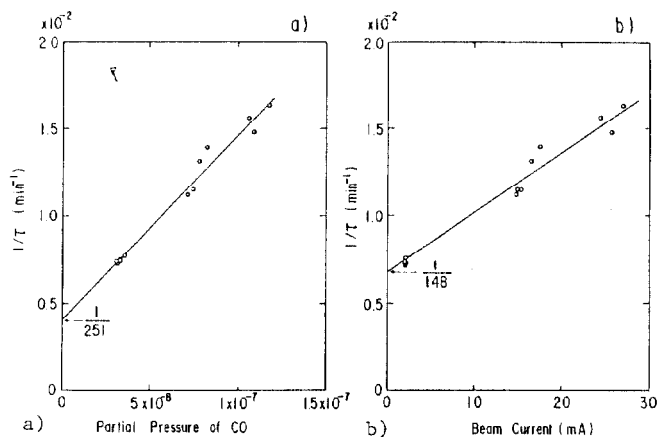


Fig.4, Reciprocal of beam lifetime as a function of a) partial pressure of CO and b) beam current.

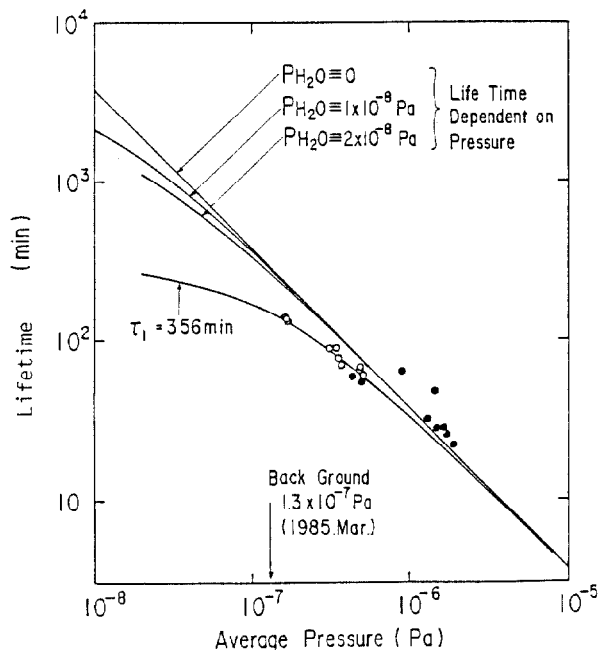


Fig.5, Beam lifetime as a function of average pressure.

430 min, CO. CO is the most dominant and, therefore, the most important to reduce. In Fig.5,  $\tau_2$ , as obtained from Eq.(2), is shown as a function of the gate pressure. To increase  $\tau$ , it is necessary to improve the base pressure and to reduce  $\Delta P$  in the AR.

#### Wall Current

In electron storage rings, the electron beam excites wall currents inside the beam chambers. Therefore we took care to insure a continuous current flow. The aluminum alloy gate valves provide continuous current flow. The valves have dual flat mirror surface seals and employ differential pumping. No influence of the wall current was observed on the gate valves. On the other hand, ordinary Viton seal type gate valves showed significant pressure deterioration during operation. This is because the valves have a discontinuous structure for the flow of wall current. The valves were subsequently exchanged to the dual flat mirror surface seal type.

Similar problems were observed for a current transformer CT and the ceramic chambers. CT is a coaxial type cavity and has a gap of 5 mm in order to cut the wall current. Pressure deterioration of  $10^{-2}$  Pa was ob-

served at more than 20 mA in a single bunch. This CT was eliminated and a new type, which had a ceramic chamber, has been designed. The ceramic chambers for the kicker magnets are rectangular blocks with an oval apertures. A Ti-Mo film was coated on the inside surface to provide for a continuous current flow. The thickness of the film is 2  $\mu$ m so that the magnetic field of the magnets can penetrate in the hole. Heating (50-80 °C) was observed at the discontinuities between the Ti-Mo film and the aluminum bellows which are at the ends of the chambers. They were repaired by an improved evaporating source of Ti-Mo.

#### Cooling System and Corrosion

A cooling circuit consists of aluminum pipes servicing 2 bending and 2 quadrupole magnets. Maximum power at the bending chambers is about 1 KW/m at 20 mA and 6.5 GeV. The aluminum bellows at each side of the bending chamber receives about 100 W. To protect the 0.3 mm thick aluminum bellows, a water cooled aluminum absorber (5 mm  $\phi$  x 5 mm high) was welded inside the chamber to shadow the bellows. Since the critical energy at 6.5 GeV is 28 KeV, the penetration depth is 2.8 mm which absorbs 83 % of the power. The effect of the absorber has been confirmed by a test using a high energy electron beam with an equivalent power and penetration depth. In fact, no thermal troubles were observed in the bellows.

The temperature of the cooling water for the AR is controlled to be in the range between 10 and 30 °C. When the temperature was set lower than the dew point, the surface of aluminum chambers was covered with moisture. Moisture together with dust, particularly concrete dust causes the formation of hydroxides. Thus, the temperature of cooling water was set higher and the humidity was lowered. An influence of humidity was observed on the outer surface of a 80  $\mu$ m aluminum extraction window which is down stream of the Mo internal target. The aluminum hydroxide on the surface can be made by the interaction of  $\gamma$ -rays with humidity and  $NO_x$ . Therefore the window was changed to a 0.3 mm thick Be<sup>x</sup>-plate which was covered with helium gas. Some of the high voltage connectors for the SIPs and DIPs deteriorated because of humidity. It was estimated that humidity accelerated abnormal discharges in the connectors carbonizing the insulator and oxidizing the metal. This was overcome by reducing the humidity in the AR tunnel. Therefore humidity control is important.

#### Conclusions

The all-aluminum, ultra-high vacuum system for the TRISTAN AR, has been operated for two years without any substantial difficulties. High reliability and performance for aluminum vacuum systems have been demonstrated. Much valuable information has been learned and applied both to improve the operation of the AR and to the design and construction of the TRISTAN main ring.

#### References

- [1] K. Narushima et al., "Outgas of the Al alloy vacuum chamber," J. Vac. Soc. Jpn., 25, 172-175, 1982.
- [2] H. Ishimaru, "All-aluminum alloy ultrahigh vacuum system for a large-scale electron-positron collider," J. Vac. Sci. & Technol., 2, 1170-75, 1984.
- [3] H. Watanabe et al., "Control of the TRISTAN vacuum system," Proc. 5th Symposium Acc. Sci. & Technol., 1984, 256-258.
- [4] S. Noguchi et al., "12-cell DAW structures in the TRISTAN AR," *ibid.*, 111-113.
- [5] C. Falland et al., "2 years operational experience with the PETRA vacuum system," 8th Intern. Vac. Conf., 1980, 385-389.
- [6] H. Kitamura et al., "Status of the vacuum system in the PF electron storage ring," Proc. 5th Symposium Acc. Sci. & Technol., 1984, 234-236.

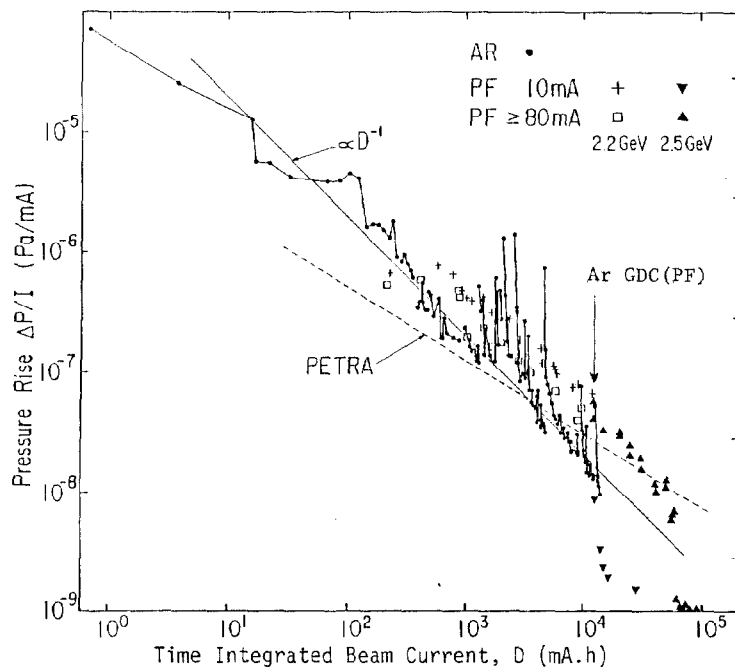


Fig. 2 Pressure rise as a function of a time integrated beam current.

$$\Delta P/I = 2.0 \times 10^{-4} \times D^{-1} \text{ (Pa/mA)}. \quad (1)$$

This is shown by the straight line in Fig. 2. The dashed line in Fig. 2 shows results from PETRA<sup>5</sup>, where the chambers were prebaked at 150 °C and precleaned by Ar discharge. Results similar to our AR data were observed at the KEK photon factory PF, where baking was done before the first operation. We don't understand the differences in slope or in  $\Delta P/I$  between our results and those from PETRA and PF. It should be mentioned, however, that unbaked, specially extruded aluminum alloy chambers show similar characteristics as ordinary extrusions do after baking.

We have observed that  $\Delta P$  is proportional to beam current  $I$ , e.g.,  $\Delta P/I$  is constant. Also, initially,  $\Delta P/I$  is proportional to beam energy  $E$ , until  $D \approx 3$  A.h. After  $D \approx 10$  A.h, it is proportional to square root of  $E$ . This suggests that the influence of beam energy decreases as  $D$  increases.

Relative amounts of residual gas species with beam were found to be 38( $H_2$ ), 12( $CO$ ), 6( $CO_2$ ), and 1.5( $H_2O$ ) at 1.7 mA.h. These ratios are constant in the pressure range between  $1.3 \times 10^{-4}$  and  $6.5 \times 10^{-6}$  Pa. These ratios have remained nearly constant over the 2 year period of operation.

#### Beam Lifetime

The beam lifetime, as a function of the time integrated beam current, is shown in Fig. 3, a). If we neglect the energy dependence, the data can be explained qualitatively as follows. When the current is low,  $\Delta P$  is small, in this case the lifetime  $\tau$  is determined solely by the base pressure. The base pressure changed with time as shown in Fig. 3, b), improving by one order of magnitude. During this time,  $\tau$  improved by only about a factor of 7. This discrepancy suggests that  $\tau$  includes a pressure independent factor. When the current is high, it is expected that  $\tau$  will be proportional to  $D$ . Increases in  $D$  of about one order of magnitude track well with similar increases in  $\tau$ .

A more quantitative analysis can be made. The relationships between  $\tau^{-1}$ ,  $I$ , and partial pressure of  $CO$   $P_{CO}$  at  $D = 13.3$  A.h are shown in Fig. 4, a) and b), Fig. 5 shows  $\tau$  as a function of average pressure. At 13.3 A.h, the following relationships are observed:

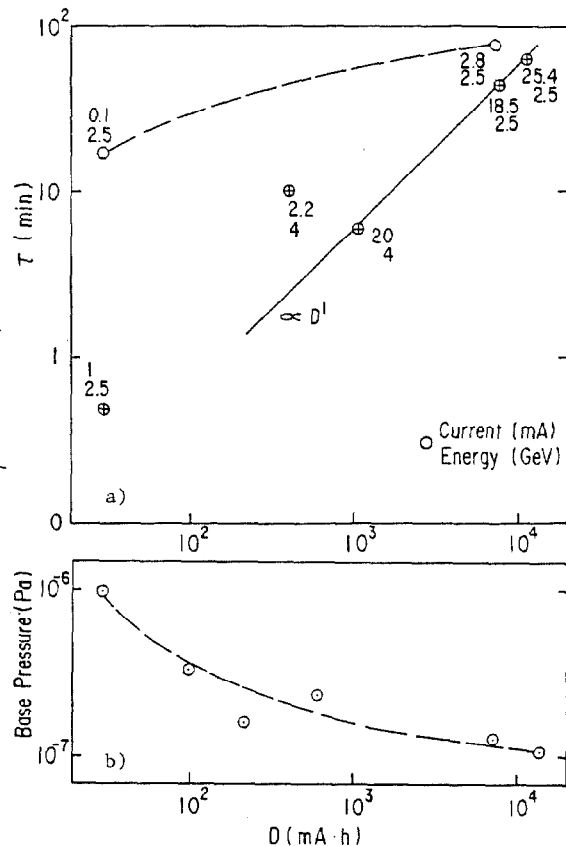


Fig. 3, a) Beam lifetime and b) base pressure as a function of a time integrated beam current.

$$\begin{aligned} P_{H_2} &= 3 \times P_{CO} \text{ (peak heights), independent on } I, \\ P_{H_2O} &= 2 \times 10^{-8} \text{ Pa, constant,} \\ \text{Base pressure} &= 1.3 \times 10^{-7} \text{ Pa.} \end{aligned} \quad (2)$$

The lifetime  $\tau$ , with no pressure rise due to beam, is given by Eq. (3),

$$1/\tau = 1/\tau_1 + P_{H_2O}/A_{H_2O} + P_{H_2}/A_{H_2} + P_{CO}/A_{CO}, \quad (3)$$

where  $\tau_1$  is independent of  $I$  and pressure.  $A$  are intrinsic constants of the residual gas species and are proportional to the sensitivity of the gauge and the  $Q$  mass filter. Using the Eq. (2), we see that the first two terms in Eq. (3) are independent of  $P_{CO}$  and other two terms are dependent on  $P_{CO}$ . Extrapolating  $P_{CO} = 0$ , we find the sum of the first two terms to be  $1/251 \text{ min}^{-1}$  as shown in Fig. 4, a). If we assume that the main influence of the residual gas on the beam is due to brems-strahlung, we can fix the ratios of the constants  $A$ , and calculate each term in Eq. (3). This gives  $\tau_1 = 356 \text{ min}$ . This value may depend on parameters related with the operation of the AR, in a way that we do not yet understand.

The lifetime  $\tau$ , which takes account of the pressure rise due to the beam current  $I$ , is given by

$$1/\tau = 1/\tau_2 + (\Delta P_{H_2O}/A_{H_2O} + \Delta P_{H_2}/A_{H_2} + \Delta P_{CO}/A_{CO}) \quad (4)$$

$$1/\tau_2 = 1/\tau_1 + 1/\tau_0.$$

$\tau_2$  is found to be 148 min by extrapolating to  $I = 0$  in Fig. 4, b). This gives  $\tau_0 = 252 \text{ min}$ , a value which agrees well with the value obtained from Eq. (3) using the ratios for the constants  $A$  and Eq. (2). This agreement suggests that these ratios among the constants  $A$  are reasonable. Partial lifetimes due to the various residual gas species are: 1800 min,  $H_2$ ; 1100 min,  $H_2O$ ;